19th Australasian Tunnelling Conference – Acosta-Martínez, Stewart and Hudson-Smith (Eds.)

Stability Analysis of a Nozzle Headwall considering interaction with adjacent piles: Insights from Sydney Metro West

Ivy Zhang
Senior Engineer, SMEC, Australia

Ali Golshani
Principal Engineer, SMEC, Australia

ABSTRACT: The Sydney Metro West Western Tunnelling Package (WTP) consists of 9 km of twin TBM tunnels linking Sydney Olympic Park and Westmead. At eastern end of Parramatta station box, 16 m-long nozzles connect the station box to future TBM tunnels.

A critical challenge involves excavating nozzles within 4.6 meters of a commercial building's pile foundations, necessitating tunnel-pile interaction analysis to verify headwall stability and primary support adequacy.

This study applies 2D and 3D Finite Element Modellings (FEM) to assess these interactions, incorporating geological conditions, structural geometry, and construction sequencing. Analytical verification methods and numerical modelling results were compared, evaluating their applicability for the site's multi-layered geology, bolt lengths and shear resistance.

Findings highlight 3D FEM's superiority in capturing spatial complexities, while affirming the applicability and conservatism of analytical approaches. The research offers practical guidance on integrating analytical and numerical techniques to enhance design accuracy and risk management in tunnel engineering.

1 INTRODUCTION

The plan view of the Parramatta (PTA) nozzle enlargement mined tunnel is shown in Figure 1 (a). Nozzle enlargement tunnels will be excavated from within the Parramatta station. The total length of the nozzles is 16m with the RT01 nozzle located on the southern side and the RT02 located on the northern side.

Building No. 25 Smith Street is located to the south-east of the nozzles and is marked out on the top left corner of Figure 1. The P10 pile—which carries the highest ultimate pile load—and the C1 pile are the two closest foundation elements to the nozzle headwall. Given their proximity, they are considered the most critical analyses cases regarding interaction between piles and headwall.

This paper analyses the stability of the nozzle headwall and the adequacy of headwall primary support prior to TBM running tunnel breakthrough, with particular focus on the influence of piles. An analytical approach, along with 2D and 3D FEM were undertaken, and the results were compared.

This analytical method, based on Pells (2001), was refined to place greater emphasis on rock bolt capacity. This capacity was evaluated in detailed considering rock properties, bolt type and bolt spacing, grouting strength, and most importantly, the length of the bolts embedded within the potential rock failure wedge. The method for determining the rock bolt capacity within a failure wedge followed the approach proposed by Anagnostou (2014). In addition, the shear resistance provided by rock bolt 'dowel action' was also considered, using the methodology proposed by Pells (2002).

The 2D and 3D FEM models undertaken using RS2 and RS3 programs considering the anticipated local geology. In the 2D model, a support pressure (derived from calibration of monitoring data) was applied on the nozzle crown and headwall to simulate the effect of the supporting system. In the 3D model, the ground support system was installed as per design and the excavation of nozzles were modelled following the proposed construction sequence. Stability conditions of the nozzle headwall

obtained from 2D and 3D models were compared with results from the analytical method. Results and findings are presented in Section 6 of this paper.

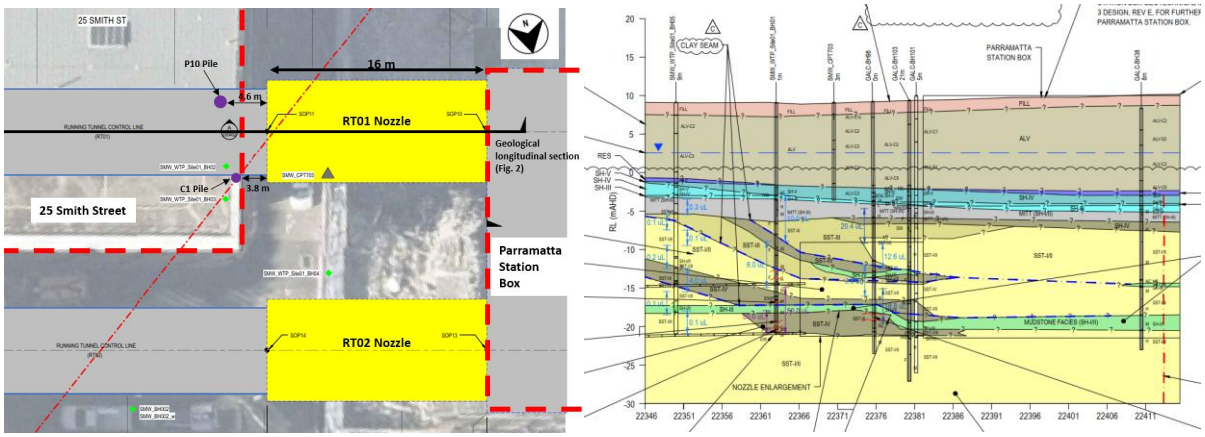

(a) (b)

Figure 1. (a) Parramatta nozzle enlargement plan view; (b) Parramatta station box and nozzle enlargement – RT01 control line geological longitudinal section.

2 SITE GEOLOGY

The geological longitudinal section of the PTA nozzle enlargement tunnels aligned along the RT01 nozzle control line is presented in Figure 1 (b). PTA nozzle enlargement tunnels are underlain by a thick layer of Alluvium (around 10 m thick) followed by Ashfield Shale Class IV to Class I/II located on top of the nozzle crown. Nozzle headwall mainly intersects with declined Sydney Sandstone Class IV – II dipping towards the nozzle opening.

3 ANALYTICAL DESIGN METHOD

3.1 *Headwall stability*

The headwall stability analysis was carried out applying the limit state design principle. The proposed support system is deemed acceptable if the following principal equation is satisfied:

$$FoS = R/D. \tag{1}$$

where R is the total resistance force acting on the failure surface; D is the total driving force happened on the surface; FoS is the resulting factor of safety. The typical failure mechanism of a headwall is presented in Figure 2 (a).

R represents the total resisting force, comprising the headwall support force F_s provided by rock bolts; the shear and friction resistance at the base of the wedge and the additional shear resistance R_b mobilized by rock bolts intersecting the failure surface where the "dowel action" takes place.

D represents the total driving force, comprising the self-weight of the wedge G; the full overburden load from upper underground material above the tunnel crown V_s and the pile load V_{pile}.

$$R = \left[G \cdot cos\alpha + F_s \cdot sin\alpha + (V_s + V_{pile}) \cdot cos\alpha\right] \cdot tan\Phi + F_s \cdot cos\alpha + c \cdot H/sin\alpha \cdot w + R_b \tag{2}$$

$$D = G \cdot sin\alpha + (V_s + V_{pile}) \cdot sin\alpha \tag{3}$$

where α = failure angle between failure surface and horizontal level; Φ = internal friction angle on the failure surface; c is cohesion on the failure surface; H is tunnel height; w is tunnel width.

3.2 *Headwall support force F_s*

The headwall support force F_s is determined by the total capacity of all rock bolts installed in the headwall.

Generally, the support force provided by each bolt depends on the following factors:

- The bolt's factored tensile capacity (F_t),
- The diameters of the grouted borehole (d) and the bolt (d_b),
- The bond strength between the soil and grout interface (τ_m),

- The bond strength between the grout and bolt interface (τ_g),
- The anchorage length within the failure wedge (a) and
- The anchorage length ($L-a$) in the bedrock ahead of the inclined failure surface ($L-a$) as shown in Figure 2 (b).

The surface reinforcement equation introduced by Anagnostou (2014) is given as:

$$F_s = N \cdot \min\left[F_t, \max\left(\min\left(d\tau_m, d_b\tau_g\right)\pi a, F_p\right), \min\left(d\tau_m, d_b\tau_g\right)\pi(L-a)\right]. \quad (4)$$

This equation accounts for the factored rock bolt tensile capacity (F_t), the failure of the anchor face plates (F_p) and the shear failure at the bolt-grout-rock interface both inside the failure wedge (2nd term) and outside of the failure wedge (3rd term). The support force (F_s) provided by each rock bolt is determined by the minimum of these three terms.

For a given bolt length (L) installed in a specific rock layer with a determined bolt spacing, once the failure surface angle α is known, a_i and $L-a_i$ can be calculated at each row of rock bolts. Using Equation (4), the minimum of these three terms can be determined and the total support force (F_s) is the sum of the capacities of each individual rock bolt.

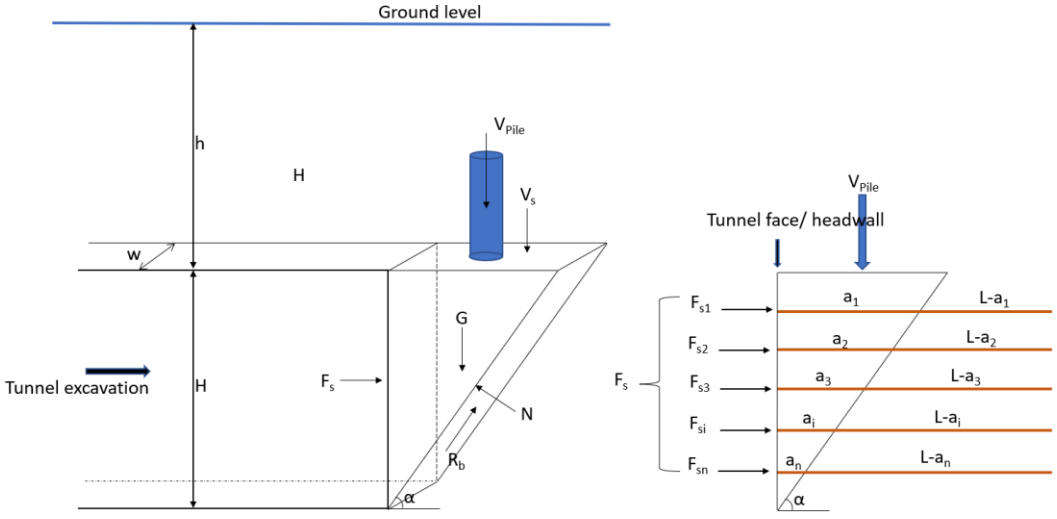

(a) (b)

Figure 2. (a) Headwall failure mechanism; (b) rock bolt support force F_s distribution on tunnel headwall.

3.3 *Rockbolt additional shear resistance* R_b

In wedge stability analysis, grouted rock bolts provide a 'dowel action' that is activated by the movement of the wedge. This dowel action only becomes active once the wedge begins to move, offering an additional resisting force along the potential sliding plane, thereby enhancing the overall stability of the system.

Research published by Pells (2002) specifically addressed the contribution of rock bolt to the 'cohesive' strength of the joint, and the contribution of tension mobilized in the bolt to the frictional resistance developed on the joint plane.

Pells (2002) suggests that the presence of a reinforcing bolt or cable increases the shearing resistance of the joint by the following mechanisms:

1. An increase in shear resistance due to the lateral resistance developed by the bolt via 'dowel action' – force R_1,
2. An increase in normal stress as a result of prestressing of the bolt – force R_2,
3. An increase in normal stress as a result of axial force developed in the bolt from dilatancy of the joint – force R_3, and
4. An increase in normal stress as a result of axial force developed in the bolt from lateral extension – force R_4.

R1 can be considered as increasing the cohesion of the joint, while R2, R3 and R4 contribute to increasing the frictional component of the interface strength by increasing the effective normal stress on the interface. Therefore, the force acting normal to the joint plane is given by:

$$N = R_2 + R_3 + R_4 \quad (5)$$

So that the additional shearing resistance generated by each rock bolt intersecting with the failure surface R_b is given by:

$$R_b = R_1 + N \cdot tan\Phi_j \quad (6)$$

where Φ_j is the friction angle of the rock wedge failure surface. Detailed calculation steps for R_1, R_2, R_3 and R_4 were presented in Pells (2002). In this paper, shear displacement = 1 mm was adopted in the failure surface to calculate the additional shear resistance.

4 2D FINITE ELEMENT MODELLING

4.1 *Ground model*

The longitudinal cross section of the RT01 control line was developed using Rocscience RS2 program and is presented in Figure 3 (a). The model followed the geological long section shown in Figure 1 (b). As this paper focuses on the nozzle headwall stability, the excavation of Parramatta station box and the future RT01 TBM running tunnel were not incorporated in the model.

Support pressure applied on the nozzle crown and headwall simulated the effect of the installed supporting system. The pressure magnitude was calibrated to match the displacement values observed in real-time monitoring.

A total ultimate pile load of 10.3 MN was applied. This approach was adopted to represent a conservative (worst-case) loading condition.

The nozzle long section shown in Figure 3 (a) was modelled following the proposed construction stages as outlined below:

- Initialization stage
- Application of ground floor surcharge
- Excavation of the basement and pile, followed by concrete placement.
- Application of ultimate pile load of 10.3 MN
- Excavation of the nozzle top heading and application of support pressure
- Excavation of the remaining benches and invert, with support pressure applied.

Based on the project's geotechnical interpretive report (GIR) and the actual nozzle alignment orientation, the major in-situ stress (σ_H) was applied out-of-plane and the minor in-situ stress (σ_h) was applied in-the-plane (as shown in Figure 3 (a)).

Rock mass parameters were based on Project's GIR and are presented in Table 1. In this analysis, tunnel scale parameters were used. Hoek-Brown failure criterion was adopted for Sandstone Class II & III, Mittagong (Shale I/II) and Shale III. More-Coulomb failure criterion was adopted in Sandstone IV, Shale IV and soil layers.

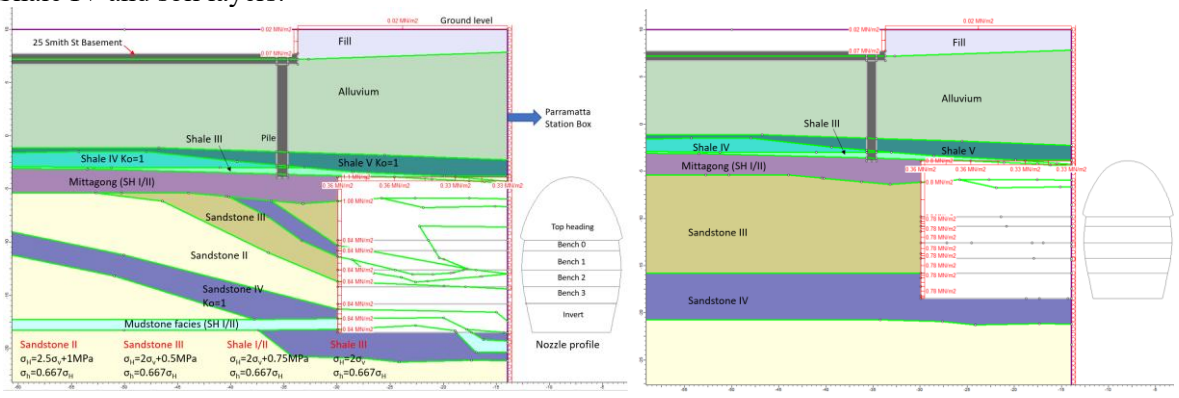

(a) (b)

Figure 3 (a) RS2 model RT01 longitudinal cross section and nozzle cross section; (b) RS2 sensitivity case.

Table 1 – Characteristic rock mass parameters

Design approach	Parameter	SST II	SST III	SST IV	SH II	SH III	SH IV	SH V
Substance	Intact UCS (MPa)	25	15	10	15	8	4	1
	Poisson's ratio, ν	0.25	0.25	0.25	0.25	0.25	0.25	0.3
Tunnel scale rock mass	Mass modulus (MPa)	2000	1000	500	1000	300	110	15
	GSI	65	55	45	50	40	30	20
	m_b	3.438	2.406	-	1.341	0.939	-	-

Hoek-Brown[1]	s	0.0205	0.0067	-	0.0039	0.0013	-	-
	a	0.502	0.504	-	0.506	0.511	-	-
Mohr-Coulomb[2]	C' (kPa)	-	-	200	-	-	90	40
	Φ (°)	-	-	40	-	-	25	15
	T (kPa)	-	-	10	-	-	0	0

Notes:

1. Damage parameter 'D' of 0, assumes minimal disturbance to rock mass surrounding tunnel.
2. Normal stress range of 0 to 2 MPa assumed.

4.2 *Shear strength reduction approach*

The Shear Strength Reduction (SSR) option in RS2 can automatically perform a finite element slope stability analysis and compute a critical strength reduction factor for the model. The critical strength reduction factor (SRF) is equivalent to the "safety factor".

SSR analysis was conducted in RS2 model to evaluate the headwall stability and determine the critical strength reduction factor of the nozzle headwall. Three typical excavation stages (top heading, bench 0 and full-face excavation) were considered. For each stage, the headwall toe displacement was plotted against the corresponding SRF. The point at which the displacement curve begins to increase noticeably is interpreted as the onset of failure, with the corresponding SRF taken as the Factor of Safety (FoS) for the headwall. Detailed RS2 analysis results are summarised in Table 3.

5 3D FINITE ELEMENT MODELLING

5.1 *Ground model*

A 3D model was developed, incorporating the geology, nozzle excavation, and the basement and piles of the 25 Smith Street building. As in RS2 model, the Paramatta station box and the future TBM running tunnels were not incorporated in the model. The high in-situ stress major direction was assigned along the nozzle transverse direction. Ultimate pile pressures were applied at the pile toes as shown in Figure 4 (a). The material properties used in the model are presented in Table 1.

The proposed nozzle supporting system was incorporated in accordance with the anticipated ground conditions (Figure 4 (b)):

- Nozzle crown: 300 mm steel fiber reinforced shotcrete (SFRS).
- Nozzle sidewalls:
  - Bench 0: 4m long CT bolts on pillar side and 3 m long on the non-pillar side;
  - Bench 1/2/3 and invert: 4m long GFRP bolts on pillar side and 3 m long on the non-pillar side;
- Nozzle RT01 headwall: 9m long CT bolts on the top heading area; 6m long GFRP bolts on the benches and invert. 100 mm steel fiber reinforce shotcrete (SFRS) on the headwall.
- Nozzle RT02 headwall: 4m long CT bolts on the top heading area; 4m long GFRP bolts on the benches and invert. 100 mm SFRS on the headwall.

The stages considered in the RS3 modelling were the following:

- Initialization stage
- Excavation of basement and piles, followed by concrete application
- Application of piles ultimate pressure at pile toe
- Excavation of RT02 nozzle and installation of support in a single stage
- Excavation of RT01 nozzle top heading, with shotcrete application and installation of headwall rock bolts
- Excavation of RT01 Benches and Invert and installation of the corresponding rock bolts and shotcrete on the sidewall and headwall at each excavation stage

5.2 *Shear strength reduction approach in RS3*

Shear strength reduction analysis was also performed in RS3 to assess the stability of the RT01 headwall. After the nozzle excavation was completed, the headwall toe displacement was plotted against the strength reduction factor. When the displacement curve begins to noticeably increase, the headwall failure is considered to have occurred, and the corresponding SRF is taken as the factor of safety for the RT01 headwall in the 3D condition.

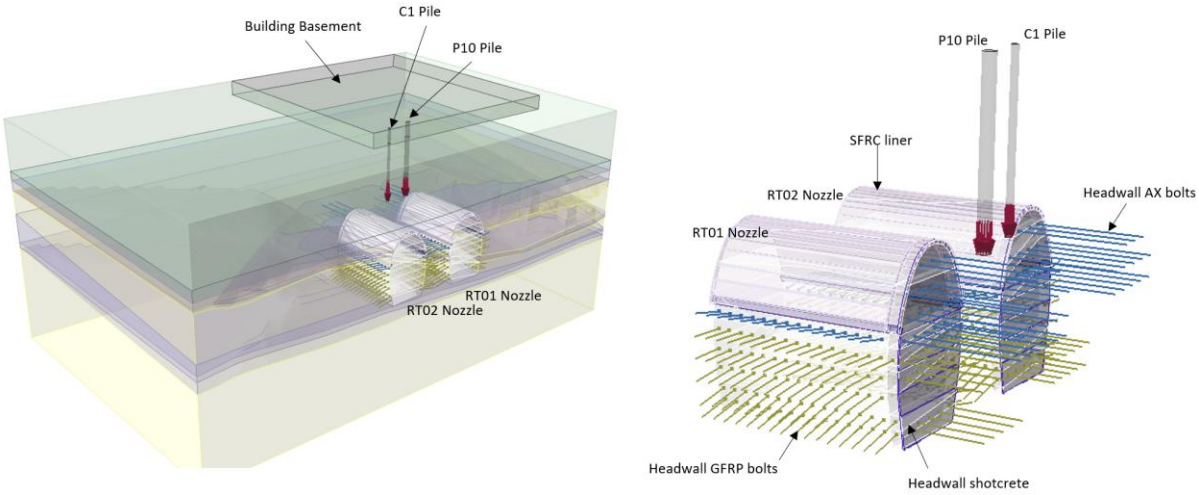

(a) (b)

Figure 4 (a) RS3 model overview; (b) RS3 model two nozzles with supporting system.

6 ANALYTICAL METHOD AND FEM MODELLING RESULTS

The FoS obtained for the nozzle headwall, determined using both the RS2 shear strength reduction analysis and the analytical method, is summarized in Table 2.

The FoS from RS2 modelling was determined by plotting the headwall toe total displacement against SRF. The SRF at the point where the total displacement curve begins to noticeably increase was selected as the headwall FoS.

The analytical method was calculated using the SMEC in-house spreadsheet. The detailed calculation process is presented in Section 3. By inputting specific parameters such as geological layer thickness, bolt spacing, bolt length, and bolt design capacity, the FoS for a potential wedge failure at any failure angle α can be calculated. The failure angle α must fall within a specific range that considers the pile load (as shown in Figure 2 (b)). Thus, the headwall FoS is the minimum value within this α range.

Table 2. Analytical method and FEM modelling results

Run ID	Modelling scenario	FoS from RS2	FoS from RS3	Analytical method FoS without/ with additional shear resistance (as a counter check to FEM)
Run1	Excavate till top heading level	2.0	2.3	1.8 / 2.0
Run2	Excavate till Bench 0 level	2.0	2.3	1.7 / 1.8
Run3	Nozzle fully excavate	2.7	2.9	1.6 / 1.9

The RS2 headwall toe displacement versus SRF is shown in Figure 5 (a), while the toe displacement increment sloping versus SRF is plotted in Figure 5 (b). An example of that can be seen in Figure 6 where RS3 Run1 and Run 3 results are shown.

Figure 5 (b) shows that in Runs 1, 2 and 3, total toe displacements experience significant increments at SRF values of 2.0, 2.0 and 2.7, respectively, which correspond to their respective FoS. The total displacement contour for RS2 Run 1 (Figure 6 (a)) indicates a failure surface passing from pile toe to the top heading toe at SRF=2.0. In RS2 Run4 (Figure 6 (b)), although a large toe displacement increment is observed at SRF=2.7, the total displacement contour doesn't show an obvious failure surface. This is primarily due to the geological conditions behind the headwall. As shown in Figure 3 (a), a wedge of Sandstone Class III and a declined strip of Sandstone Class IV are located behind the top heading, causing the rock to fail along this material boundary.

The RS3 model results for the toe displacement of top heading, bench 0 excavation and full-face excavation and their corresponding rate of increment (sloping) are presented in Figure 7 (a). A noticeable increase in toe displacement for top heading, bench 0 level and full-face excavation occurs at SRF=2.3, 2.3 and 2.9. Thus, FoS for top heading, bench 0 level and full-face in RS3 model were determined. RT01 nozzle full-face rock displacement passing through the RT01 control line at SRF=2.9 was presented in Figure 7 (b).

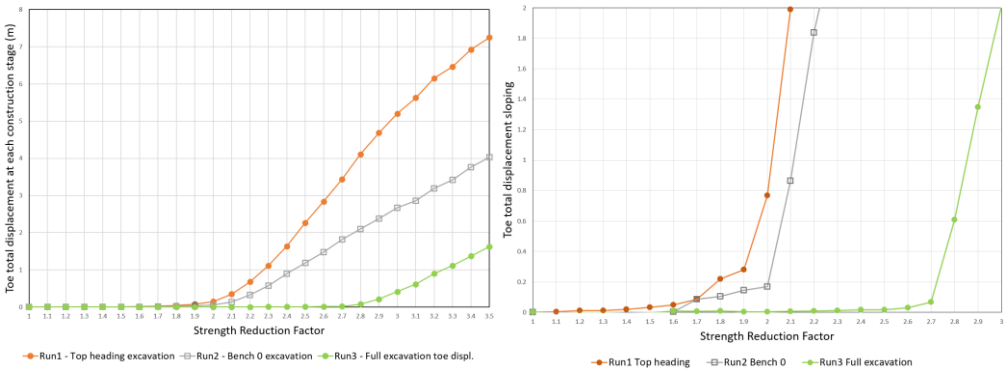

(a) (b)

Figure 5. (a) RS2 headwall toe displacement versus SRF; (b) Toe displacement sloping versus SRF.

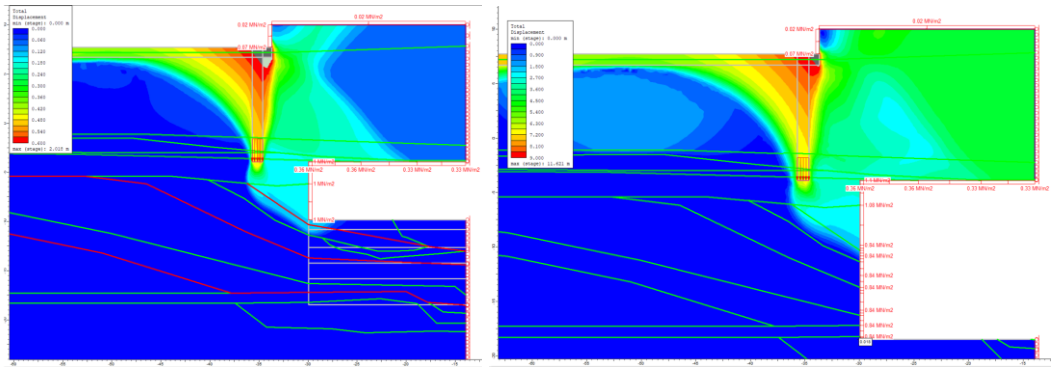

(a) (b)

Figure 6. (a) RS2 Run1 top heading displacement contour at SRF=2.0; (b) RS2 Run3 full face displacement contour at SRF=2.7.

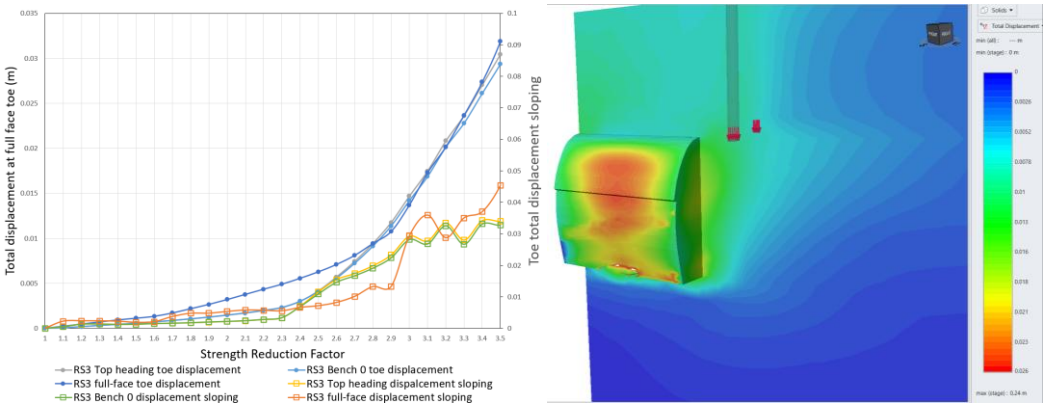

(a) (b)

Figure 7. (a) RS3 full face toe displacement and increment sloping versus SRF; (b) RS3 RT01 full face rock displacement contour at SRF = 2.9.

To assess the influence of geological geometry on headwall stability, a sensitivity analysis was conducted by modelling the ground stratification to be horizonal, instead of being inclined, as shown in Figure 3 (b). In this sensitivity case, the geology above headwall level remained unchanged, while the boundaries between Mittagong formation (SH I/II), Sandstone Class III and Sandstone Class IV were assumed to be horizontal. Sensitivity analysis results are presented in Table 3 and Figure 8. The headwall FoS under this geological configuration was determined to be 2.1. The corresponding FoS from the analytical method for the same geological setup was 1.6/1.8.

The sensitivity analysis highlights the significant role that geological shape plays in headwall stability. When the material boundary behind the headwall is horizontal, the analytical method aligns more closely with the RS2 results, although both remain slightly conservative.

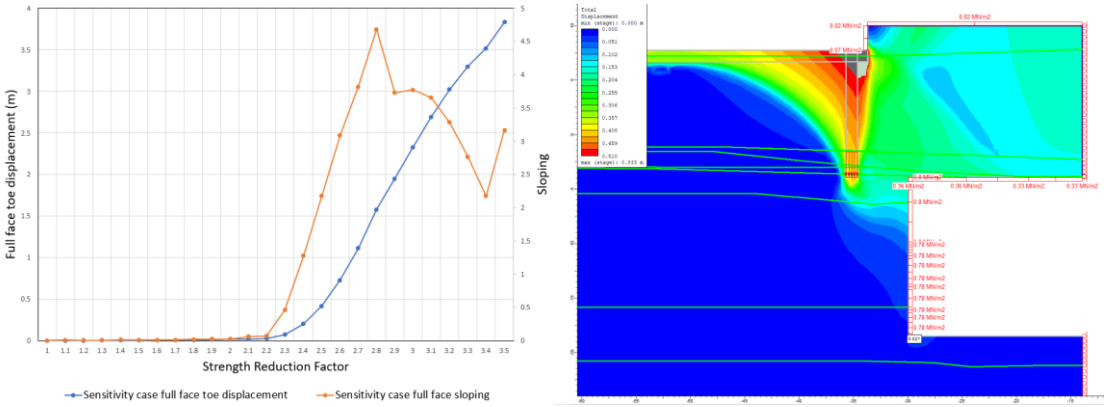

(a) (b)

Figure 8. (a) RS2 sensitivity case full face toe displacement and increment sloping versus SRF; (b) sensitivity case full face toe contour at SRF=2.2.

Table 3. RS2 sensitivity analysis results

Run ID	Modelling scenario	FoS from RS2	Analytical method FoS without/ with additional shear resistance (as a counter check to FEM)
Sensitivity case	Nozzle fully excavate	2.2	1.6/ 1.8

7 FINDINGS AND CONCLUSION

The paper compares the 2D and 3D finite element modelling with an analytical approach to assess the stability of nozzle headwalls under the load of adjacent piles.

In this paper, ground support was modelled in RS2 by applying support pressure based on back-calculations from monitoring data. This is because a longitudinal 2D model cannot accurately represent the arching effect in the tunnel transverse direction. Using the same input parameters (including pile depth, pile pressure, and geology), the RS3 model produced a similar headwall FoS to RS2 and the headwall displacement closely matched the observed displacement monitoring data, validating the RS3 modelling approach. The analytical approach is always conservative as it excludes several factors such as geological stratigraphy, in-situ stress conditions, pile shaft friction and face shotcrete. In this study, the contribution of rock bolt dowel action was incorporated when a failure surface is formed. The results indicate that accounting for this dowel action leads to an increase in the headwall FoS by approximately 0.2 to 0.5.

When geology consists of moderate to weak strength material and is inclined towards the tunnel opening, the failure surface is more likely to develop along the material boundary, regardless of the tunnel opening size. To assess the influence of geological geometry on headwall stability, a sensitivity analysis was carried out using RS2, where the geological layers were adjusted to a horizontal configuration. Under this scenario, the analytical results aligned more closely with the RS2 result but remained conservative. This highlights the importance of considering the actual geological profile and applying sound engineering judgement when evaluating failure surfaces. A larger tunnel opening does not necessarily imply a lower FoS.

8 REFERENCES

G. Anagnostou, P. Perazzelli. Analysis method and design charts for bolt reinforcement of the tunnel face in cohesive-frictional soils.

Pells, P. J. N. Development in the design of tunnels and caverns in the Triassic rocks of the Sydney region. International Journal of Rock Mechanics and Mining Sciences, Vol 39, pp 569 -587 2002.

Pells, P.J.N. A Note on Rockbolt Design for Load Supporting Ledges in Hawkesbury Sandstone. Aust. Geomechanics, Dec 2001.